800-yr-long records of annual air temperature and precipitation over southern Siberia inferred from Teletskoye Lake sediments

Ivan Kalugin [a,*], Andrei Daryin [a], Lyubov Smolyaninova [a], Andrei Andreev [b],
Bernhard Diekmann [b], Oleg Khlystov [c]

[a] Institute of Geology and Mineralogy SB RAS, Pr. Ak. Koptyuga 3, RU 630090, Novosibirsk, Russia
[b] Alfred-Wegener-Institute for Polar and Marine Research, Telegrafenberg A43, D-14473 Potsdam, Germany
[c] Institute of Limnology SB RAS, Ulan-Batorskaya 3, RU 664033 Irkutsk, Russia

Abstract

A unique 800-yr-long record of annual temperatures and precipitation over the south of western Siberia has been reconstructed from the bottom sediments of Teletskoye Lake, Altai Mountains using an X-ray fluorescence scanner (XRF) providing 0.1-mm resolution timeseries of elemental composition and X-ray density (XRD). Br content appears to be broadly correlative with mean annual temperature variations because of changes in catchment vegetation productivity. Sr/Rb ratio reflects the proportion of the unweathered terrestrial fraction. XRD appears to reflect water yield regime and sediment flux. Sedimentation is rather continuous because annual clastic supply and deposited mass are the same. The artificial neural networks method was applied to convert annual sedimentary time-series of XRD, Br content, and Sr/Rb ratio to annual records of temperature and precipitation using a transfer function. Comparison of these reconstructed Siberian records with the annual record of air temperature for the Northern Hemisphere shows similar trends in climatic variability over the past 800 yr. Estimated harmonic oscillations of temperature and precipitation values for both historical and reconstructed periods reveal subdecadal cyclicity.
© 2007 University of Washington. All rights reserved.

Keywords: Teletskoye Lake; XRF scanner; Sub-millimeter time series; Temperature and precipitation records

Introduction

Lake sediments provide archives of various parameters that can be correlated to climatic oscillations such as seasonal temperature and humidity. Different transfer function techniques are commonly applied in order to reconstruct high resolution paleo-temperature and humidity (e.g., Kumke et al., 2004 and reference therein). Similar to tree-ring methods (Cook and Kairiukstis, 1990; Cook et al., 1998; Briffa, 2000), these techniques are calculated as optimal linear or nonlinear regressions calibrated on recent meteorological data.

However, geochemical records from many modern European and Asian lakes cannot be directly correlated with meteorological data within densely populated areas, because of anthropogenic pollution. Human impact has greatly increased in recent times, coincident with the period of instrumental measurements of the last 150–200 yr (e.g., Lottermoser et al., 1997; Ramrath et al., 1999; Fernandez and Grimalt, 2003). However, the pollution issue is not significant for the mountain lakes of Siberia, remote from centers of anthropogenic pollutions, although even here various pollutant compounds can be detected (Gavshin et al., 1999). For such lakes, a correlation of their sedimentological and geochemical (inorganic) parameters with instrumental measurements of the last 150 yr is possible. Teletskoye Lake is especially promising for the inference of a robust record of climatically driven solid detrital supply from the catchment, because there is no agriculture in the area, and population density does not exceed one person per square kilometer (Atlas, 1969).

An 800-yr history of annual temperatures and atmospheric precipitation in the south of western Siberia has been reconstructed from a deep-water site in Teletskoye Lake, Altai Mountains (Kalugin et al., 2005). Its sedimentation is rather

* Corresponding author. Fax: +7 383 333 2792.
  E-mail address: ikalugin@uiggm.nsc.ru (I. Kalugin).

continuous as it is strongly controlled by the close relationship between both annual clastic supply and deposited sediment mass (Selegei et al., 2001; Kalugin et al., 2005).

Processes of sedimentation in the lake have been previously investigated in order to choose a representative site suitable for the high-resolution paleolimnological studies. In total, about 70 short cores (up to 180 cm long) were taken over the years throughout the lake basin. The correlation of sedimentary sequences by magnetic susceptibility allowed the tracing of marker layers within the northern basin across a distance of more than 10 km. The magnetic susceptibility record and similarities in lithology of the collected sediment cores reveal uniform sedimentation within the northern basin where the studied core was collected (Fig. 1).

Gamma spectrometry measurements of ^{137}Cs and ^{210}Pb have been done for several cores collected in vicinity of studied core Tel 2001-02. Our previous results show that sedimentation rates vary between 1 and 1.4 mm/yr for wet sediments in the northern part of the lake (Bobrov et al., 1999). The lowest average values (0.69–1.04 mm per yr) in the northern basin are revealed near the western slope, between 230 and 265 m water depths. Eastward they increase up to 1.5 mm per yr at the 270–310 m depth level, probably due to coastal erosion and prevalent suspended matter movement along the east shore (Selegei and Selegei, 1978). An average sedimentation rate of 1–2 mm per yr was estimated for the core site, using a combined ^{137}Cs and ^{14}C chronology. Sedimentation rates correspond well with seasonal sedimentological supply, and have stayed rather stable for facies not impacted by turbidity currents. A qualitative model of climatic changes during the last 800 yr has been constructed using geochemical and biogenic markers, and several cold and warm climate fluctuations were identified, which corresponded to global climatic events (Kalugin et al., 2005).

In this paper, we make significant advances on a previous study (Kalugin et al., 2005) and report on a detailed quantitative climate reconstruction obtained by exploiting the geochemical sediment proxies from the 800-yr finely laminated sequence from Teletskoye Lake (Fig. 1). Application of rapid and highly
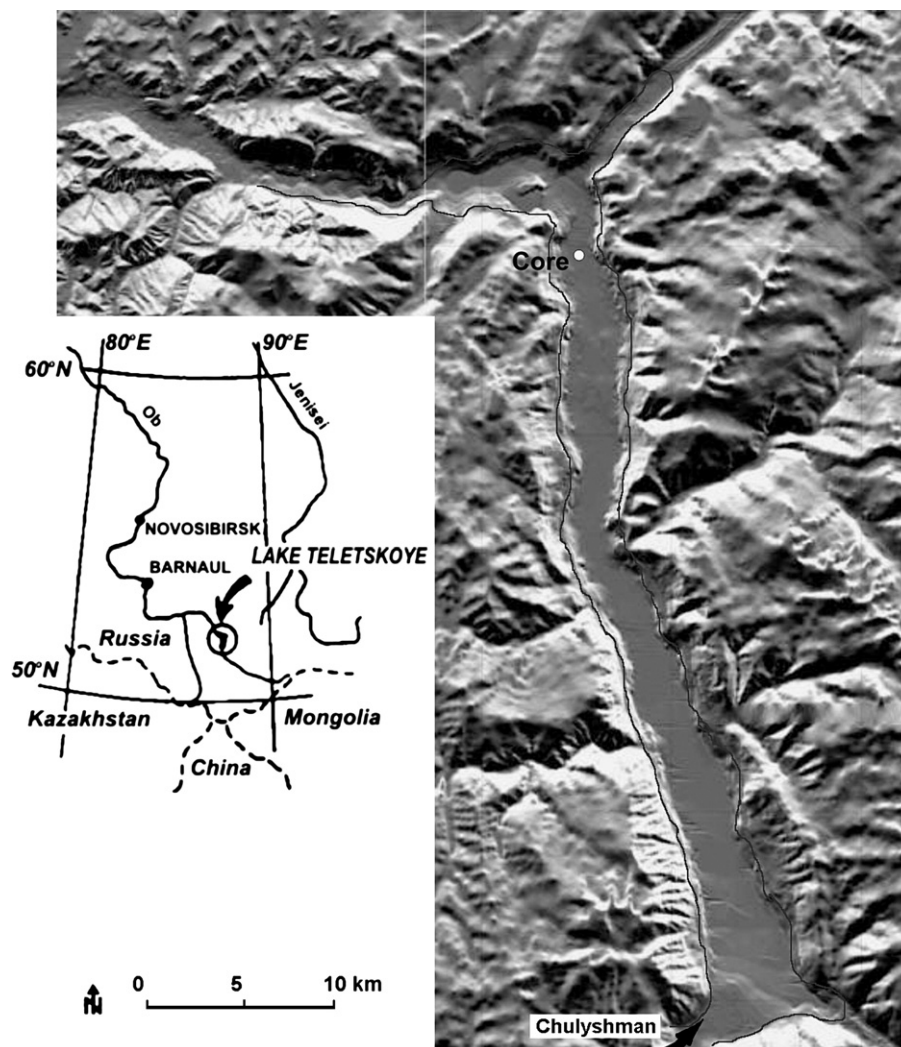

Figure 1. Location of Teletskoye Lake. Shaded relief demonstrates topography and bathymetry of the Teletskoye Lake basin area, which have been combined to provide a general digital model (Dehandschutter et al., 2002). The underwater steep slope looks like a narrow band between shoreline and plane bottom (for complete bathymetry see Selegei et al., 2001). Key core site and Chulyshman River are marked.

sensitivity scanning analysis on sediment cores (Tel 2001-02 and Tel 2002) in the Siberian Center of Synchrotron Radiation, Novosibirsk, allowed the determination of elemental composition at 1-mm resolution (Daryin et al., 2005; Goldberg et al., 2005). Construction of a quantitative age-based model has been done after correction for compaction of the upper sediment layers (Kalugin et al., 2005) and confirmed by AMS ^{14}C dating from the bottom of the core (this work). Artificial neural networks (ANN) have been applied to reconstruct past climate changes using sediment proxies.

Lake and study site

Teletskoye Lake is located in the taiga zone of the NE Altai region (51°39′N, 87°40′E, 434 m a.s.l.). It is a tectonic lake, deep, long, open and has a dimictic mixing regime (for other limnological parameters, see Table 1). More than half of water input to the lake is provided by spring and summer floods after seasonal snow melt. Chulyshman River (Fig. 1) supplies about 70% of annual water inflow into the southern part of the lake, and all other small rivers and streams provide the majority of the remaining 30% (precipitation on the lake surface only accounts for <2% input). The ratio of total water volume (41.06 km^3) to

Table 1
Lake Teletskoe parameters and sedimentation indices

Parameter	Measured values [a]
Length on median	47.3 km
Width	3.51–5.2 km
Depth	mean 206 m, max 323 m
Surface area	166.1 km^2
Area enclosed within 250-m isobath	83.68 km^2
Capacity	34.16 km^3
Annual water input for 1975–1990	6.048 km^3
Lake water, suspended matter content. Annual mean for 1979–1996 from 3 stations	3.2 mg/l
Input water, suspended matter content. Annual mean for 1979–1996, Chulyshman River	18.6 mg/l
	Estimated
Lake water, suspended matter content by water input, mean for 1979–1996	3.3 mg/l
Lake water, suspended matter content by sediment mass, mean for 1948–1997	6.2 mg/l
Residence time of suspended matter, by lakewater balance for 1979–1996	0.98 yr
Residence time of suspended matter, by sediment mass deposited in 1948–1997	1.94 yr
Bottom sediments	
Water volumetric content, mean of 422 samples, core Tel 2004	63.10%
Volumetric weight, mean of 422 samples, core Tel 2004	1.63 g/cm^3
Accumulation rate for wet sediment, core Tel 98-01, Tel 2001, Tel 2002 (one location), by ^{137}Cs, [210]Pb	1.09 mm/yr (north basin)
Accumulation rate for wet sediment, core Tel 2001, by [14]C	1.06 –1.08 mm/yr

[a] From Selegei and Selegei (1978); Selegei et al. (2001).

annual inflow (7.56 km^3) is 5.4. Biya River is the only outlet with an annual discharge 6.9 km^3, and evaporation is insignificant (Selegei and Selegei, 1978). Balance estimations show that the annual suspended load to the lake is almost completely deposited during a year (Kalugin, 2001).

Generally, climate in the lake region is temperate-continental (Selegei et al., 2001); the influence of the Siberian High prevails in winter, and westerly influence increases in summer. For reconstructions presented here, cores Tel 2001-02 and Tel 2002 were collected in northern part of longitudinal Basin (51°42.90′ N, 87°39.50′E) from a water depth of 325 m.

Methods and materials

Several sediment cores up to 250 cm long were collected from the deepest part of the lake in 2001, 2002 using a 6-cm-diameter piston, a 10-cm-diameter gravity core and a box corer. The cores were initially examined to determine physical properties, including lithology, mineralogy, and geochemistry. Grain size measurements were done using a Mastersizer S modular particles size analyzer (Malvern Instruments). Total carbon content was analyzed by CNS Elementer Vario El III. In addition, pollen-inferred climate change has been studied in the core Tel 2001-02, the details of which are presented by Andreev et al. (this issue).

Here we report on the geochemical approach for detailed sedimentological study, based on Lotter et al. (1997) and Neumann et al. (1997). Geochemical time-series of elemental composition, together with X-ray density (XRD) measurements were obtained by X-ray Fluorescence Analysis using Synchrotron Radiation (SRXFA) technique. In contrast to traditional methods of discrete analysis (Baryshev et al., 1989), the continuous XRF scanning technique applied to freshly opened longitudinally split sediment cores has been applied in order to obtain high-resolution temporal analyses. One-dimensional XRF scanning at a VEPP-3 storage ring at the "Baikal" SRXFA station in the Budker Institute of Nuclear Physics, Novosibirsk, has been used for the detection of elemental composition of studied cores (Zolotarev et al., 2001). Records of 28 elements with 1-mm scanning resolution were obtained from the cores simultaneously. Both the ratio of coherent/incoherent scattering and X-ray density were registered for each sample. Three energies of incident photons provided all measurements. The 15-keV band was used for elements determination from K to Br. The spectra of Rb, Sr, Y, Zr, Nb, Mo, Th and U were measured with 23 keV, while Cd, Sn, Sb, I, Ba, La and Ce spectra were measured with 45 keV beams. This method has great potential for wet sediment cores because many elements can be analyzed simultaneously without additional sub-sampling.

The applied age model and assignments of the respective ages of individual laminae were based on previously published data (Kalugin et al., 2005). To develop a ^{137}Cs-derived timescale for Tel 2002 core, thicknesses of individual, sampled layers were first recalculated into 'dry depth', using the relationship $H_{dry} = H_{wet}(1 - V_{water}/V_{wet})$, where V denotes volume and H denotes thickness. This procedure is necessary because of the down-core decrease in water volumetric content

from ca. 80% in the top sediments to ca. 60% for sediments at 25–30 mm and lower (Table 1). The depth of layer with maximum measured ^{137}Cs content was correlated to AD 1963, the year of maximum global fallout. Finally, after summing up the corrected (decompacted) thicknesses of all measured layers, and from the average ^{137}Cs-derived sedimentation rate, we are able to estimate that the top of the thick marker layer at ca. 90 cm core depth is approximately AD 1210±25 (Kalugin et al., 2005).

Small plant remains were also washed out of the marker layer at the 95–97 cm depth (core Tel 2002) and used for the AMS ^{14}C dating. The ^{14}C date, 897±43 cal yr BP (KIA26018) (calendar age is AD 1160 within two-sigma range: (AD 1027–1220) confirms the ^{137}Cs chronology. Our AMS ^{14}C dating is likely to be accurate because, as it was tested by Oldfield et al. (1997), single terrestrial detritus in carbonate-free lake water and sediments would provide real ^{14}C content and radiocarbon dates close to the true age of the sediment. Moreover the short period (5–6 yr) of full water exchange (Selegei and Selegei, 1978) in the lake excludes any age shift due to reservoir effects.

Data processing included calculation of basic statistics, correlation, and routine time-series analysis. Artificial neural networks (ANN) (Veelenturf, 1995) were used for reconstruction of annual temperature and precipitation by sediment properties (Smolyaninova et al., 2004). In general, connections between climatic parameters and the properties are rather complicated, and all geospheres are ensembles of some open nonlinear systems. Thus, the method of linear regression employed for climate reconstruction (e.g., Mann et al., 1998) may be not quite adequate, or at least can be improved upon. Moreover, linear regression is very sensitive to time series being complete and continuous, thereby making additional problems for many paleolimnological reconstructions. Consequently, ANN techniques more commonly used in related disciplines (e.g., Guiot et al., 1995; Keller et al., 1997; Woodhouse, 1999; Racca et al., 2001; Belgrano et al., 2001) are used here, although for lake sediments there are particular features that need to be addressed.

ANN employs nonlinear multivariate regression with regulating smoothness of the outlet function, whose form depends on neural network structure. In this study, ANN with two layers was used. Its algorithm of functioning is $\alpha_i = \sum_j x_{ij} \sin\left(\sum_k y_{jk} A_k\right)$, where α_i=outlet signal of neural network, A_k=inlet operation factors, x_{ij}, y_{jk}=operation factors to be modifying with the procedure of training. This procedure is the program of optimization, where functional of training error is minimized. Algorithm "back propagation" (Rumelhart et al., 1986; Werbos, 1990) and method conjugate gradients were applied for optimization.

Instrumental records from AD 1840 to 1996 from the Barnaul weather station located at 200 km NW of the Teletskoye Lake were also used in this work. From this data source, correlation coefficients between annual and winter air temperatures are as high as 0.89–0.92. Summer temperatures are less variable, and ca. 75% of warming in the 20th century is associated with cold seasons (i.e. winter and spring) (see also

Table 2
Correlation of annual T and P with element content and its ratios in sediments

1880–1991	T	Br/XRD	Sr/Rb	XRD	Br	Sr
Br/XRD	0.41					
Sr/Rb	0.28	0.63				
Br	0.41		0.59	−0.73		
XRD	−0.35		−0.82			
P	−0.26	−0.27	0.08	−0.02	−0.30	
Rb						−0.64

r=0.24 for p=0.01 and r=0.19 for p=0.05.

Klimenko, 2001; Goldberg et al., 2005). Annual temperature and precipitation have a negative correlation ($r=-0.26$ ($p<0.01$) calculated for 1880–1996 yr (Table 2).

Results and discussion

Sediment lithology

The sediments of Teletskoye Lake consist of laminated (Fig. 2), carbonate-free clayey silt with mean 42% of primary moisture. They contain ca 7% of water in dry weight, 1.14% of TOC (measured as total carbon content), and 2.5% of biogenic SiO_2 (Kalugin, 2001). Boundaries between laminae are distinct, transitional or not well expressed. However, based on lithological characteristics there are three types of laminae: (1) the dark gray-green silty layers, independent or occurring in the bottom part of rhythmites; (2) light-grey clayey individual layers, as well as mid- and top zones of rhythmites; and (3) beige and dark brownish-green clays with organic substance usually occupy top of rhythmical bands and series. Thickness of visibly homogenous layers varies over a wide range from 0.5 mm up to 2.5 cm (Kalugin et al., 2005), which seems to be proportional to the duration of turbid water.

Some intervals within the sediment column are thinly laminated that according to the age model represents annual layers or varves. This is close to the classical type of varves, such as described in Finland lakes (Antti et al., 2005). Here cyclical alternation of laminae with similar lithological features is observed in thin sections, and the cyclical nature of XRF records demonstrates that these laminations are annual in nature (Fig. 3).

The terrigenous component of the sediments consists of an illite and chlorite matrix containing non-rounded clastic grains of quartz, feldspar, biotite, amphibole, garnet, epidote, ilmenite–magnetite and metamorphic shales. The biogenic component consists of a combination of plant remains, diatom frustules, pollen and charcoal particles.

The species compositions of diatoms in the lake water and in the sedimentary deposits are not similar. Benthic taxa are dominant in the sediments (Skabichevskaya, 1998) in spite of a very narrow littoral region around the lake shore (see Fig. 1). This observation, together with the increase of the ^{137}Cs inventory in sediments close to inflows (Kalugin, 2001), confirms an allochtonous source of terrigenous and biogenic material in the bottom sediments. Authigenic mineralization is
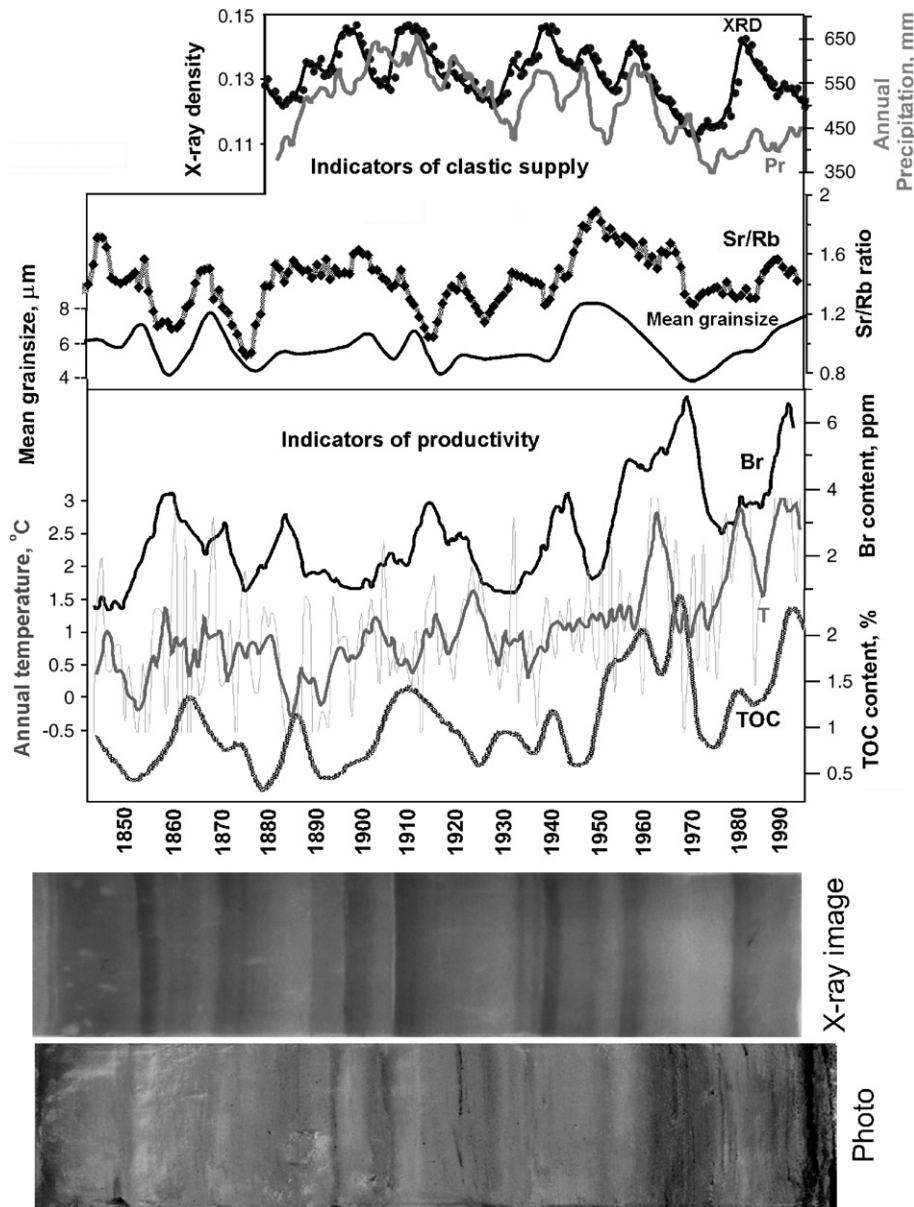
Figure 2. Comparison of Teletskoye Lake sedimentary proxy responses in core Tel 2001-02 plotted alongside the instrumental climate record over AD 1840–1996 from Barnaul weather station. Upper sketch shows proxy records in Tel 2001-02 (from bottom to top: TOC content, Br content, Sr/Rb ratio and mean grain size, X-ray Density), compared with absolute values of annual air temperature (T) and precipitation (Pr). XRD profile decouples from annual precipitation in the interval 1840–1880. Note the good agreement between grain size and Sr/Rb ratio as indicators of clastic supply. Lower sketch—combined positive radiographic image (top) and photo (bottom) for the uppermost part of cores Tel 2001-02 and Tel 2002, respectively. Dark layers on radiographic image are denser and correspond to peaks on XRD profile, but they are light on the photo because of the lack of organic pigment. Conversely, organic reach layers are light on X-ray image and dark on the photograph, which coincide with the peaks on TOC and Br profiles.

represented by small clusters of vivianite, and by hydroxides of iron and manganese marking a sub-bottom oxidized zone of 15–25 mm thick.

The weathering rate of bedrock in watershed is low and consists mainly of mechanical destruction and formation of secondary illite–hydromicaceous minerals. Thus, the variability of measured sediment properties is determined by mineral and organic components. These variations are rather smooth on the concentration curves in all cores, reflecting stable sedimentation regime, and provide a possibility for continuous reconstructions.

Accumulation of sediment mass

The sedimentation in the northern deep (320 m) within longitudinal part of the Lake (Selegei et al., 2001) is described by Kalugin et al. (2005) (Table 1). This basin accumulates fluvial input from Chulyshman River and lateral inflows—Kokshi, Chelyush, Chili, Korbu, and other small rivers, all draining the surrounding high mountainous area. The total contribution of these rivers and lateral inflows is approximately 80%. The total annual sediment load entering to longitudinal sedimentary basin is calculated as a product of suspended matter content and 80% of
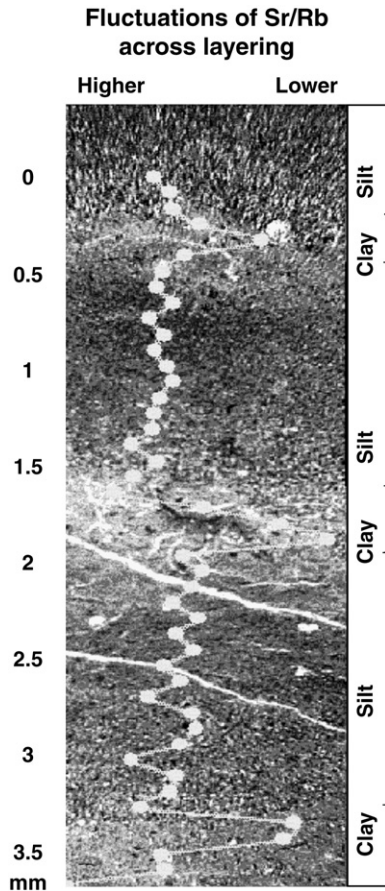
Figure 3. Fluctuations of Sr/Rb across layering, sample Tel 96-05/89–93 cm. Thin section was analyzed by SRXFA with a scanning step of ca. 80 μm.

total annual water inflow (see Table 1) and equals 112,500 tonnes. This mass is enough for settling of an annual layer of wet sediment 0.84 mm thick within the main sedimentation area bordered by the 250-m isobath, which is ca. 83.68 km^2, excluding the area of steep slopes where sedimentation is insignificant. This value is close to the average sediment accumulation rate in Teletskoye Lake of 1.1 mm per yr (see above).

Proxies from XRF scanner data

It is evident that sediments of Teletskoye Lake contain information about climate and environmental conditions in which they were deposited, and the objective here is to select the most appropriate parameters for quantification of these conditions. ANN logic and structure allow using any parameters connected with climate. Usually the pair correlation between proxies and climatic series is stronger—the conformity between transfer function and initial climatic parameters is better. Nevertheless, there is no stringent rule for selecting optimal arguments of function. A minimum error for both training and testing data series may serve a formal criterion of the best approximation over the training interval.

To calculate transfer functions for temperature and precipitation, we have selected only the best understood sedimentolo-

gical characteristics, most notably Br content, X-ray density and Sr/Rb ratio. They have high analytical accuracy and sufficient variability, and they also are connected with sedimentary facies and climate according to geological conception. Selected sedimentological characteristics describe essential mineralogical and physical properties of sediments, and reflect a proportion of main terrigenous phases such as organics and clastic fractions from different sources.

The time-series of Br concentration almost parallel the content of TOC, measured as total carbon content in carbonate-free sediments (Fig. 2). The maxima of TOC coincide with high Br value and dark-colored, lower X-ray-density intervals of deposits (Fig. 2). The minima of TOC coincide with low Br concentration and seem to occur during colder climatic conditions. This relationship is based on the certain degree of agreement between the TOC, Br and annual temperature profiles during the past 160 yr collected at the Barnaul weather station (Fig. 2) (estimated pair correlation: $r_{TOC-T} = 0.44$, $r_{Br-T} = 0.4$ ($p < 0.01$) for series in Fig. 2). A similar positive correlation between organics and annual temperature was obtained on varved series in Finland (Antti et al., 2005).

X-ray density (XRD) signal has maximum values in silt–sand containing layers, lower values in clay, and the lowest values in organic-rich sediments. XRD seems to be the parameter reflecting water yield regime and sediment flux. With the exception of the past 20 yr, XRD appears to be closely correlated with annual precipitation from AD 1880 to 1980 collected at the Barnaul weather station (Fig. 2).

The light and wet organic matter can be considered as porosity in a solid mineral matrix, and therefore sediment density and Br content have trivial negative correlation. As the density reflects the bulk composition, and bromine is defined in weight percent units, Br/XRD ratio can be used as a dimensionless parameter—namely, a productivity index for the catchment. In our case it gives positive dependence with temperature (Table 2). However, Br and XRD have been separately used for estimations after testing by ANN procedure.

Sr and Rb contents reveal a negative correlation in the sediments (Table 2) connected with different parent minerals for each of them: illite for Rb, and Ca-feldspar for Sr. Roughly, Sr and Rb reflects clay content versus silt, which allows use of
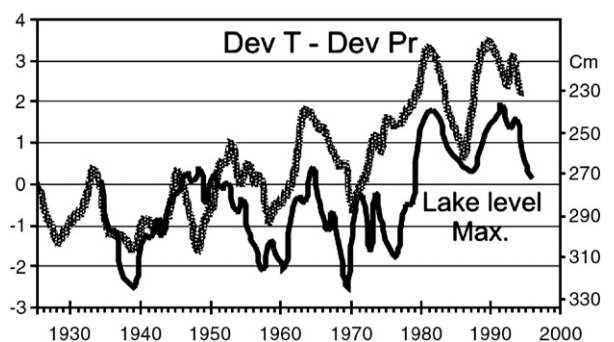

Figure 4. Lake level change (right axis) in comparison with drought index (Dev T–Dev P) as the difference between temperature and precipitation deviations (left axis).

Sr/Rb ratio as a dimensionless parameter of sediment response. In Fig. 2, the dependence of the Sr/Rb ratio on grain size is evident. Fig. 3 demonstrates cyclical distribution of Sr/Rb ratio across microlayering in thin section, and reflects the dependence of geochemical signal with lithology of annual layers. The bottom part of annual layers is mainly composed of silt, and the percentage of clay fraction increases up-layer in clayey units. The Sr/Rb signal follows lithological composition, and the value of the signal is high in silty laminae, although it significantly decreases in clayey laminae (Fig. 3). The correlation coefficient between Sr/Rb and median grain size in the range from < 2 to 28 μm is good ($r=0.68$ ($p<<0.01$) for the dataset of 390 samples confirming visual thin-section observations.

A good correlation of Sr/Rb ratio with grainsize and clay particle concentration is found in surficial sediment samples from different locations of the lake. For example, the Sr/Rb ratio measured in the sediments near the Chulyshman River mouth has a value of 2.42 but decreases to 1.92 in samples from deeper facies with water depths of between 55 and 105 m (concomitant with lower concentration of coarse

grains). Values of Sr/Rb ratio collected from deltas of small rivers of the northern basin of the lake increase up 4.0 but show a decline to 1.72 in the surficial sediment at water depths below 250 m. According to Stoke's law and observations, the concentration of clay particles in bottom sediments of lakes increases with the water depth and distance from shoreline. Consequently, the value of Sr/Rb is higher in coarse-grained sediments representing unweathered terrestrial matter, but it is lower in clayey organic-rich sediments. Thus the Sr/Rb ratio reflects the proportion of the unweathered terrestrial fraction and may be used as an index of a terrestrial sediment flux under weak weathering conditions within this high mountainous region.

Lake level and drought index

Dependence of a hydrological mode on a climate can be expressed by direct correlation between lake level measurements and the water-inflow between AD 1975 and 1990 (Selegei et al., 2001). There is also a significant negative correlation between the maximal (flood) level measured
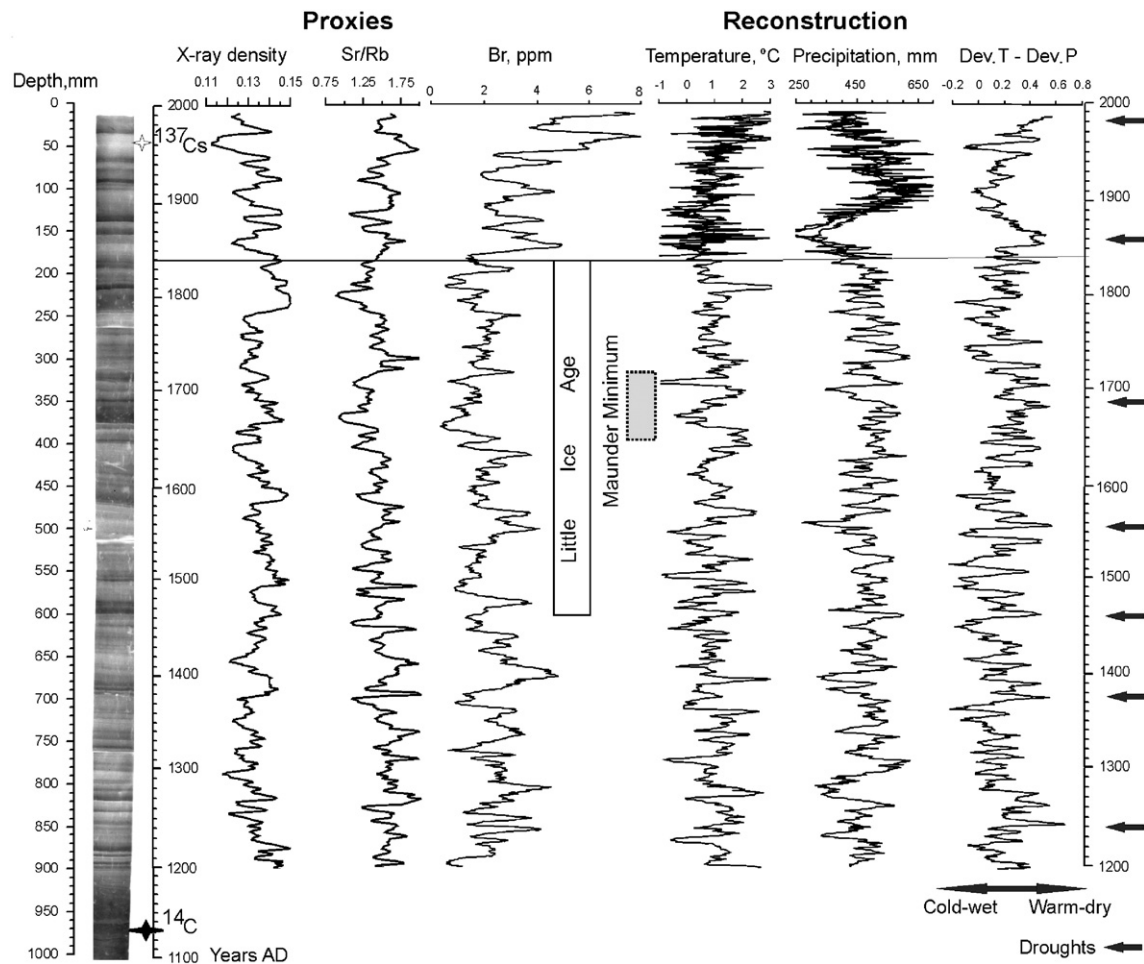

Figure 5. Reconstructed annual temperature, precipitation and drought index (Dev. T–Dev. P) profiles for the interval AD 1200–1991, together with measured sediment parameters and X-ray positive image of core Tel 2001-02 (dark bands represent higher density, see also adjacent XRD profile by XRF scanning). Solid lines are 5-yr moving averages, shaded lines=annual series of T and P for instrumental period AD 1840–1991. Asterisks mark positions of samples dated by [137]Cs (AD 1963) and [14]C (897±43 cal yr BP).

between AD 1930 to 1996, and a combination of normalized deviations from a long-term average (Dev. T–Dev. P, Fig. 4). In other words, the seasonal flood water is high in cool and wet years, but it falls during the hot and dry periods. Variations of a material drift are also connected with the change from dry to wet years (e.g., Inman and Jenkins, 1999). Thus, variability of humidity and/or a runoff controlled by joint influence of temperature and precipitation can be represented by Dev. T–Dev. P values (drought index) on an annual time-scale.

Reconstruction

A method using artificial neural networks (ANN) was applied to this study. Extrapolated annual temperature and precipitation records until AD 1210 were calculated from measuring data taken during the period AD 1840–1996. To this

Table 3
Correlation coefficients (r) between proxies and air temperature (AD 1840–1991 yr) depended on neurons number (N) and spectral density of outlet function (p) (see text)

N	p	r		
		Br	Sr/Rb	XRD
15	1	0.51	0.448	−0.504
200	10	0.514	0.383	−0.462
200	100	0.47	0.293	−0.421
200	1000	0.409	0.303	−0.33

$r = 0.21$ for $p = 0.01$.

end, functions $T = f$ (Br, XRD, Sr/Rb) and $Pr = f$ (Br, XRD, Sr/Rb), where T is the average annual temperature, Pr is the annual precipitation, Br is the content of Br, Sr/Rb is the ratio of Sr and Rb contents, were constructed.

Annual temperature, precipitation records and difference between their deviations have been restored for the interval from AD 1210 to 1991 (Fig. 5). The data from the uppermost 1.5 cm of the sediment have not been used for estimations because of semi-liquid aggregative state and anomalous Mn enrichment. Training root-mean-square error of the test-examples over the interval AD 1840–1991 is 4.6×10^{-6} °C for temperature and 0.25 mm for precipitation. From comparison of the segments on the reconstructed temperature profile, the early phase of modern warming from AD 1875 to 1965 appears to be similar to the latter stages of the Little Ice Age from AD 1730 to 1810 (Fig. 6A). The present trend towards arid conditions can be traced from ca. AD 1910, while the precipitation record from ca. AD 1845 to 1990 may be considered as an analogue of duration AD 1260–1390 in the past (Fig. 6B). Peaks on the Dev. T–Dev. P profile seem to mark drought events because increase of the value towards warm–dry condition (see Fig. 5).

An additional approach is considered here on the basis that the air temperature is related with proxies present in the lake sediment record. Pair correlation coefficients between inlet parameters and temperatures are rather low: 0.398 ($p < 0.01$), −0.326 ($p < 0.01$), and 0.078 ($p = 0.416$) for Br, XRD, and Sr/Rb, respectively, over the historical period. We therefore attempted to define which annual temperature periodicities are the most influential in determining proxy variability. To do this neural networks were trained by regulating the outlet function smoother. The degree of smoothness depends on superposition of neurons number (N) and value of spectral density of outlet function (P). Three steps are followed:

(1) Some neural networks with various values N and P were trained under number of year to define value any of the chosen parameters. As a result, some variants of the initial time series smoothing were obtained. Neuronet smoothing is similar to polynomial procedure, since outlet function is superposition of sinusoidal neuron functions.

(2) Further, values of pair correlation between the received time series and initial data of temperature for a historical period AD 1840–1991 were determined (Table 3).
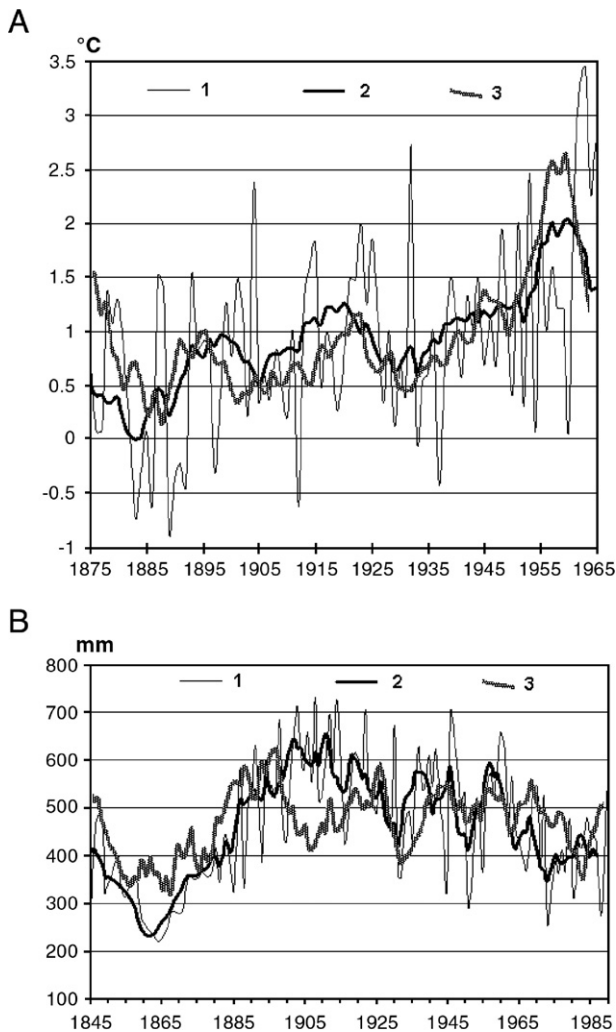

Figure 6. (A) Early phase of modern warming (AD 1875–1965) combined with period of AD 1730–1810. 1—annual temperature on Barnaul weather station, 2—the same, smoothed by 5-run average, 3—reconstructed annual temperature (this work) on duration of AD 1730–1810 smoothed by 5-run average. (B) Precipitation record from AD 1845 to 1990 superposed with restored record in AD 1260–1390. 1—annual precipitation on weather station, 2—the same, smoothed by 5-run average, 3—reconstucted annual precipitation (this work) on duration of 1730–1810 AD smoothed by 5 run average.

(3) Series with the maximal correlation coefficient were chosen for reconstruction by ANN (see underlined values in Table 3). Initial temperature reconstruction was also optimally smoothed by a 15-neuron network with a spectral density of 10. In that case, correlation between the chosen series and temperature for the period AD 1840–1991 considerably increases: 0.968, − 0.955, and 0.859 for Br, XRD, and Sr/ Rb, respectively.

As well as in the detailed version, target dependence (transfer function) is obtained by training neural network of 500 neurons. Difference consists only in values of arranged parameters.

A generalized version is shown in Fig. 7. It is not detailed, but 100-yr and 50-yr cycles can be traced through the record. Teletsk temperature trend appears to be similar to global and regional reconstructions (e.g., Jones et al., 1998; Mann et al., 1998; Crowley, 2000; Yang et al., 2002). A global cold period, the Little Ice Age with Maunder minimum, is clearly designated, as well as global warming during the 19–20th centuries.

Climatic cycles

The spectral Fourier analysis of time series was performed to determine cyclicity of annual temperatures and atmospheric precipitation . Identified periodicity for the instrumental records of ca. 19–21 and 11.5 yr (Table 4) corresponds to normal harmonics of helio-geophysical processes in the Northern Hemisphere (Berri, 1993). At the same time, periodicity of temperatures and precipitation tested together by cross-correlation on the standardized initial data are concordant, in spite of weak negative correlation (see Table 2). We then analysed time series for the restored period 800 yr. Cycles of 21–22 and ca. 11 yr are evident, similar to those determined for the instrumental data (Fig. 8, Table 4), although they appeared

Table 4
Cyclicities (yr) of temperature and precipitation in Southern Siberia

By data from Barnaul weather station for AD 1840 to 1996					
Annual air temperature	21			9.3	6.6
Annual precipitation	19		11.4	7.8	5.6

By series restored from sediment proxies for AD 1210 to 1991					
Annual air temperature	26.8	20.5	14.4	11.5	8.5
Annual precipitation	27.3	21.4	13.3	8.6	6.7

Note: Periods (yr) are estimated by spectral (Fourier) analysis.

not to be coincident with recent ones. Observed differences are likely to be related to irregular interactions between several climate forcing mechanisms over the long time interval. It is possible, for example, to expect superposition of decadal–subdecadal forcings, such as the North Atlantic Oscillation/ Arctic Oscillation, or solar activity. The role of these forcings is not yet clear in Siberia and needs work to compile data on lakes with adjacent tree ring series in the future.

Conclusions

Reconstruction of temperature and precipitation by sedimentological records from the lakes has to be based on at least two necessary assumptions. First, connection between sedimentation and seasonal/annual climatic variations should be suitable for a quantitative estimation. Second, variability of environment conditions in the past should not be essentially different from
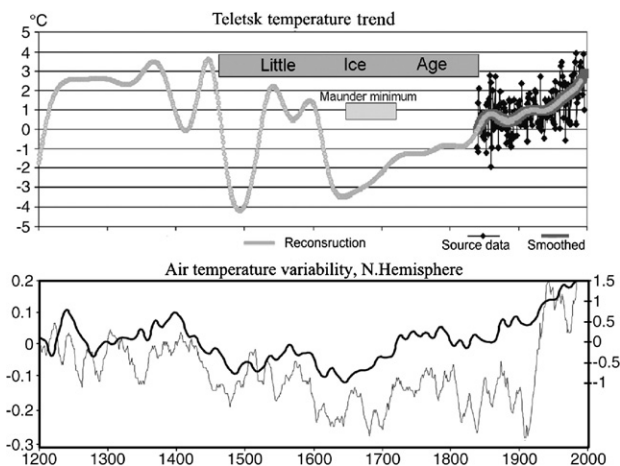

Figure 7. Reconstructed temperature trend from Lake Teletskoye sediments (upper sketch) in comparison with Northern Hemisphere temperature profile (lower sketch: thin line—temperature anomaly, relative to the AD 1961–1990 mean, left axis, Crowley, 2000) and high-resolution reconstruction from China (lower sketch: thick line—temperature anomaly, sigma units on right axis, Yang et al., 2002). Horizontal axis (years AD) is the same for upper and lower sketches.
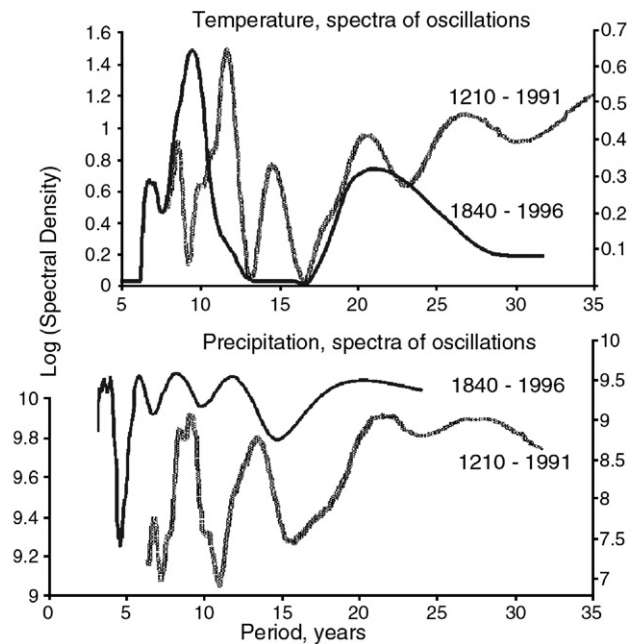

Figure 8. Decadal–subdecadal periodicity of annual air temperature (upper sketch) and precipitation (lower sketch) for instrumental period (AD 1840–1996) and for reconstruction by sediment proxies (AD 1210–1991). Vertical axis has logarithm scale for testing of statistical hypothesis of white noise, white noise curve has to look like a horizontal line. Right axis means for AD 1840–1996 (width of data window=9) and left axis—for AD 1210–1991 series (width of data window=15).

their variations during the interval of instrumental records used for the transfer function (in this study, a 150-yr record).

Applied artificial neural network (ANN) methods are possible using any primary characteristic of sediments for simulations, and thus do not require strong paired correlation between proxies and climatic parameters. Sediment properties are considered as simple nonlinear elements (or functions) forming neural networks. Elements are connected between themselves, and all information is in connection weights, which may vary. Multivariate nonlinear models are constructed on an experimental dataset by training of network with example patterns, where both inlet and outlet operation factors are known. Several natural processes are described by such functions. ANN method enables one to use not only meteorological data for training transfer function but also other possible time series such as tree ring series, isotopes and other proxies and archives.

Reconstructed ANN temperatures for the last 800 yr in southern Siberia do not contradict existing knowledge of global events during the last millennium. Our results are rather similar to dendrochronological records from Asia. Local climatic cycles of 11 (22) yr are close to (sub)decadal global cycles, such as the North Atlantic Oscillation and Arctic Oscillation and solar activity, which enables us to trace these climatic drivers back into the past. The results demonstrate the usefulness of high-resolution geochemical techniques for paleoclimate research. This scanning X-ray fluorescence analysis on Synchrotron radiation–XRF SR method has great potential for the further studies of the Holocene sedimentological archives from lakes.

Acknowledgments

References

Antti, E.K., Ojala, T., Teija, A., 2005. 10000 years of interannual sedimentation recorded in the Lake Nautajarvi (Finland) clastic-organic varves. Palaeogeography, Palaeoclimatology, Palaeoecology 219, 285–302.

Atlas USSR, 1969. Publ.House of Central administrative board of a geodesy and cartography. Moscow 1–200 (in Russian).

Baryshev, V.B., Gavrilov, N.G., Daryin, A.V., Zolotarev, K.V., Kulipanov, G. N., Mezentsev, N.A., Terekhov, Ya.V., 1989. Scanning X-ray fluorescent microanalysis of rock samples. Review of Scientific Instruments 60 (7 Pt. II), 2456–2457.

Belgrano, A., Malmgren, B.A., Lindahl, O., 2001. Application of Artificial Neural Networks (ANN) to Primary Production Time-series Data. Journal of Plankton Research 23 (6), 651–658.

Berri, B.L., 1993. Periodicity of geophysical processes and its influence on lithosphere development. Evolution of geological processes in Earth history. Nauka, Moscow, pp. 53–62 (in Russian).

Bobrov, V.A., Kalugin, I.A., Klerkx, J., Duchkov, A.D., Sherbov, B.L., Stepin, A.S., 1999. Rate of recent sedimentation in the Teletskoye Lake based on gamma-spectrometry (137Cs) data. Russian Geology and Geophysics 40 (4), 530–536.

Briffa, K.R., 2000. Annual climate variability in the Holocene: interpreting the message of ancient trees. Quaternary Science Reviews 19, 87–105.

Cook, E.R., Kairiukstis, L.A. (Eds.), 1990. Methods of Dendrochronology. Kluwer Academic, p. 394.

Cook, E.R., D'Arrigo, R.D., Briffa, K.R., 1998. A reconstruction of the North Atlantic Oscillation using tree-ring chronology from North America and Europe. The Holocene 8, 9–17.

Crowley, T., 2000. Causes of climate change over the past 1000 years. Science 289, 270–277 (14 July).

Daryin, A.V., Kalugin, I.A., Maksimova, N.V., Smolyaninova, L.G., Zolotarev, K.V., 2005. Use of a scanning XRF analysis on SR beams from VEPP-3 storage ring for research of core bottom sediments from Teletskoe Lake with the purpose of high resolution quantitative reconstruction of the last millennium paleoclimate. Nuclear Instruments and Methods in Physics Research A 543, 255–258.

Dehandschutter, B., Vysotsky, E., Delvaux, D., Klerkx, J., Buslov, M.M., Seleznev, V.V., de Batist, M., 2002. Structural evolution of the Teletsk Graben (Russian Altai). Tectonophysics 351, 139–167.

Fernandez, P., Grimalt, J.O., 2003. On the global distribution of persistent organic pollutants. Chimia 57 (9), 514–521.

Gavshin, V.M., Scherbov, B.L., Melgunov, M.S., Strakhovenko, V.D., Bobrov, V.A., Tsibulchik, V.M., 1999. 137Cs and 210Pb in lacustrine sediments from Steppe Altai as indices of dynamics of anthropogenic geochemical background change during the XX century. Russian Geology and Geophysics 40 (9), 1331–1341.

Goldberg, E.L., Grachev, M.A., Chebykin, E.P., Phedorin, M.A., Kalugin, I.A., Khlystov, O.M., Zolotarev, K.V., 2005. Scanning SRXF analysis and isotopes of uranium series from bottom sediments of Siberian lakes for high-resolution climate reconstructions. Nuclear Instruments and Methods in Physics Research A 543, 250–254.

Guiot, J., Keller, T., Tessier, L., 1995. Relational database in dendroclimatology and new non-linear methods to analyze the tree response to climate and pollution. In: Ohta, S., Fujii, T., Okada, N., Hughes, M.K., Eckstein, D. (Eds.), Tree rings: from the past to the future, Proceedings of the International Workshop on Asian and Pacific Dendrochronology. Forestry and Forest Products Research Institute Scientific Meeting Report 1, pp. 17–23.

Inman, D.L., Jenkins, S.A., 1999. Climate change and the episodicity of sediment flux of small California rivers. *J. Geol.*, Center for Coastal Studies, Scripps Institution of Oceanography, University of California, San Diego, La Jolla, California 92093–0209, U.S.A., 107, N 3, 251–270.

Jones, P.D., Briffa, K.R., Barnett, T.P., Tett, S.F.B., 1998. High-resolution palaeoclimatic records for the last millennium: interpretation, integration and comparison with general circulation model control-run temperatures. The Holocene 8 (4), 455–471.

Kalugin, I., 2001. Recent bottom fill of the Teletsk basin. In: Selegei, V., Dehandschutter, B., Klerkx, J., Vysotsky, E. (Eds.), The physical and geological environment of Lake Teletskoye. . Royal Museum of Central Africa, Ann. Sc. Geol., vol. 105. Tervuren, Belgium, pp. 263–282.

Kalugin, I., Selegei, V., Goldberg, E., Seret, G., 2005. Rhythmic fine-grained sediment deposition in Lake Teletskoye, Altai, Siberia, in relation to regional climate change. Quaternary International 136, 5–13.

Keller, T., Guiot, J., Tessier, L., 1997. Climatic effect of atmospheric CO2 doubling on radial tree growth in southeastern France. Journal of Biogeography 24, 857–864.

Klimenko, V.V., 2001. Climate of Medieval Warm Epoch in Northern Hemisphere. Moscow Energy Institute, Moscow, p. 87 (in Russian).

Kumke, T., Scholzel, C., Hense, A., 2004. Transfer Functions for Paleoclimate Reconstructions—Theory and Methods. In: Fischer, H., Kumke, T., Lohmann, G., Froser, G., Miller, H., von Storch, H., Negendank, J.F.W. (Eds.), The climate in historical times. Towards a synthesis of Holocene

proxy data and climate models. Springer-Verlag, Berlin- Heidelberg, Germany, pp. 229–244.

Lotter, A.F., Sturm, M., Teranes, J.L., Wehrli, B., 1997. Varve formation since 1885 and high-resolution varve analyses in hypertrophic Baldeggersee (Switzerland). Aquatic Sciences 59, 304–325.

Lottermoser, B.G., Schütz, U., Boenecke, J., Oberhänsli, R., Zolitschka, B., Negendank, J.F.W., 1997. Natural and anthropogenic influences on the geochemistry of Quaternary lake sediments from Holzmaar, Germany. Environmental Geology 31 (3/4), 236–247 (June 7, Q Springer-Verlag).

Mann, M.E., Bradley, R.S., Hughes, M.K., 1998. Global-scale temperature patterns and climate forcing over the past six centuries. Nature 392, 779–781.

Neumann, T., Stogbauer, A., Walpersdorf, E., Stuben, D., Schaller, T., Moor, H. Ch., Wehrli, B., 1997. Sedimentary profiles of Fe, Mn, V, Cr, As and Mo as indicators of benthic redox conditions in Baldeggersee. *Aquatic sciences* 59, 345–361, 1015–1621, Birkhäuser Verlag, Basel.

Oldfield, F., Crooks, P.R.J., Harkness, D.D., Petterson, G., 1997. AMS radiocarbon dating of organic fractions from varved lake sediments: an empirical test of reliability. Journal of Paleolimnology 18, 87–91.

Racca, J.M.J., Philibert, A., Racca, R., Prairie, Y.T., 2001. A comparison between diatom-based pH inference models using Artificial Neural Networks (ANN), Weighted Averaging (WA) and Weighted Averaging Partial Least Squares (WA-PLS) regressions. Journal of Paleolimnology 26, 411–422.

Ramrath, A., Nowaczyk, N.R., Negendank, J.F.W., 1999. Sedimentological evidence for environmental changes since 34,000 years BP from Lago di Mezzano, central Italy. Journal of Paleolimnology 21, 423–435.

Rumelhart, D.E., Hinton, G.E., Williams, R.J., 1986. Learning representations by back-propagating errors. Nature 323, 533.

Selegei, V.V., Selegei, T.V., 1978. Teletskoye Lake. Gydrometeoizdat, Leningrad, pp. 1–142 (in Russian).

Selegei, V., Dehandschutter, B., Klerkx, J., Vysotsky, E. (Eds.), 2001. The physical and geological environment of Lake Teletskoye, 2001. Royal Museum of Central Africa, Tervuren, Belgium. Ann. Sc. Geol., 105, p. 310.

Skabichevskaya, N.A., 1998. Diatom algae in the bottom sediments of the Teletstkoye Lake. Problems of paleoclimatic reconstructions in Pleistocene and Holocene 1. Publ. Institute of Archaeology and Ethnography of SB RAS, Novosibirsk, pp. 270–276 (in Russian).

Smolyaninova, L.G., Kalugin, I.A., Daryin, A.V., 2004. Technique of receiving empiri-mathematical interdependence models between climatic parameters and litologi-geochemical character of bottom deposits. Computer technology 9: Mathematic, Mechanic, Computing 3 (42), 43–46.

Veelenturf, L.P.J., 1995. Analysis and applications of artificial neural networks. Computer Science 259.

Werbos, P.J., 1990. Backpropagation through time: what it does and how to do it. Proceedings of the IEEE 78 (10), 1550–1560 (October).

Woodhouse, C.A., 1999. Artificial neural networks and dendroclimatic reconstructions: an example from the Front Range, Colorado, USA. The Holocene 9, 521–529.

Yang, B., Braeuning, A., Johnson, K.R., Yafeng, S., 2002. General characteristics of temperature variation in China during the last two millennia. Geophysical Research Letters 29, 1324.

Zolotarev, K.V., Goldberg, E.L., Kondratyev, V.I., 2001. Scanning SR-XRF beamline for analysis of bottom sediments. Nuclear Instruments and Methods in Physics Research A 470, 376–379.